Correlation of impact fracture toughness with loss peaks in PTFE

M. Kisbenyi*, M.W. Birch*, J.M. Hodgkinson and J.G. Williams
Department of Mechanical Engineering, Imperial College of Science & Technology, London SW7 2BX, UK

INTRODUCTION

There is often a close correlation between loss peaks, as measured by dynamic mechanical or electrical tests, and toughness.[1-3] Such correlations have important practical implications since the origins of loss phenomena in molecular terms are reasonably well understood; thus, in principle, tough materials may be designed on a molecular level. The picture is far from clear, however, since, although correlations are good in some materials, they do not occur in others. A detailed discussion of the problem is given by Vincent[3] who points out that there is a particularly good example of correlation in PTFE where three well defined loss peaks appear to coincide with similar peaks in Izod impact strength. In other materials, and with other tests, the peaks are less well defined, often because of interaction of phenomena such as ductile-brittle transitions, notch sharpness effects and the influence of environment.

In the programme of work described here, the deformation properties of PTFE were investigated using mechanical loss and yield stress measurements over the temperature range $-100°$ to 180°C so that frequency (and hence rate), strain amplitude and stress state effects could be studied. These results are then compared with the fracture toughness, G_c, determined over a similar temperature range and at several rates using a sharp notched impact test. A technique for determining G_c based on a fracture mechanics analysis is used[4,5] which enables accurate values to be determined which are free from kinetic energy errors and geometry effects and, as a consequence of the latter, the specimen geometry can be changed to alter the rate of the test. The detailed picture which emerges of both deformation and fracture behaviour then provides the basis for the investigation of the loss peak–toughness correlation.

STRUCTURE AND RELAXATIONS OF PTFE

PTFE is a linear chain polymer of great molecular mass containing two fluorine substituents on each main chain carbon atom. The chemical structure is shown below:

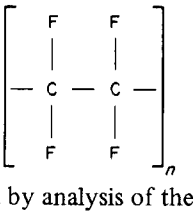

Linearity is indicated by analysis of the infra-red spectrum, and also by the highly crystalline nature of the powder produced in the polymerization reaction; crystalline weight fractions of 0.90 to 0.95 being indicated by density, infrared and X-ray diffraction measurements.

The crystalline melting point of unsintered PTFE is 332° to 346°C and of sintered material 327°C, but there are two reversible first order transitions at lower temperatures, +19° and +30°C,[6] which, taken together, involve a 1% change in density.[7] Three crystalline phases are observed at atmospheric pressure, the first below +19°C, the second between +19° and +30°C, and the third above +30°C. Below +19°C, the chain repeat distance is 16.8 Å and the chain is twisted to form a helix, thirteen carbon atoms being involved in each 180° twist. The unit cell is triclinic and essentially perfect three-dimensional order prevails. Between +19° and +30°C, the repeat distance is increased to 19.5 Å, corresponding to a twist of 15 carbon atoms in 180°. Packing on the now hexagonal lattice is somewhat disordered owing to small angular displacements of chain segments about the chain axis. Above +30°C, the preferred crystallographic direction is lost, segments being displaced or rotated along their axes by variable amounts which increase as the temperature rises. The reason for the helical structure is the necessity to accommodate the large fluorine atoms (van der Waal radius 1.35 Å). The rotation at each chain bond, with bond angles increased to 116°, relieves overcrowding and gives a shortest F-F distance of 2.7 Å.[8]

The crystallinity of PTFE has been the subject of detailed study. Estimates of the degree of crystallinity have been made by X-ray, infra-red and density methods.[9,10] Crystallinities estimated by the X-ray method range from 90% for unsintered material, 75% for fused and slowly cooled samples, to 50% for fused and rapidly quenched material. The initial high crystallinity and melting point can never be completely recovered after fusion, presumably owing to entanglements and other impediments caused by the great molecular length.

The relaxation processes occurring in PTFE have received a good deal of attention in the past and most of the work has been reviewed[11] in some detail. Mechanical and dielectric techniques indicate three loss peaks, the α peak near +150°C, the β relaxation region at around room temperature, and the γ peak at about $-90°$C.

Although there has been some uncertainty from relaxation studies as to whether the α relaxation originates in the amorphous or crystalline phase,[12,13] evidence from dilatometric and X-ray considerations[14] favours the contention that this relaxation is associated with the amorphous or disordered regions. Mechanical[12] and dielectric[15] loss peaks in the β relaxation region increase in height with increasing crystallinity, thus associating the β relaxation with the crystalline phase of the polymer. Using a similar argument

*Present address: Department of Polymer Technology, John Dalton Faculty of Technology, Manchester Polytechnic, Chester Street, Manchester, UK.

0032-3861/79/101289-09$02.00

for the γ peak,[12,15] which decreases in height with increasing crystallinity, the γ relaxation must occur in the amorphous regions.

DEFORMATION TESTS

Most of the work described here used commercially produced 6 mm sheet given no special heat treatment. Two other samples were used,* one being slow cooled after sintering, the other being quenched. Reliable values for crystallinity could not be determined by density measurements because of indeterminate void content. However, infra-red analysis indicated crystallinity values of 65% for the commercial material, with 60 and 65% for the quenched and slow cooled samples, respectively, showing some similarity in treatment between the commercial and slow cooled materials.

The basic dynamic mechanical data was obtained using a Rheovibron DDV-11 direct-reading viscoelastometer operating at 11 Hz using a simple tension stress system. Substantial corrections for end effects had to be made[16] and the resulting in-phase modulus, E', and loss factor, tan δ, data shown in *Figure 1*, are believed to be accurate. E' shows rapid changes over the three viscoelastic transitions and the loss peaks are well defined for the α transition at +145°C and for the γ at −85°C. There is a clear peak at +35°C for the β transition but with some evidence of a secondary effect at +20°C, associated with the crystal phase change. There is also evidence of a small peak at −5°C. Also shown in *Figure 1* is the tan δ peak for the γ relaxation determined at 110 Hz, which indicates the expected translation to a higher temperature (the activation energy is 18 kcal mol^{-1}) and also an increase in tan δ with frequency. This effect is confirmed by Kabin,[17] using stress wave methods, who obtained a tan δ peak value of 0.14 at −30°C for 1 MHz.

Some tests were also run on a torsion pendulum machine at 2 Hz and the loss factor is shown, together with the simple tension data (at 11 Hz), in *Figure 2*. Tan δ for simple shear is greater than that in tension, but is of similar form

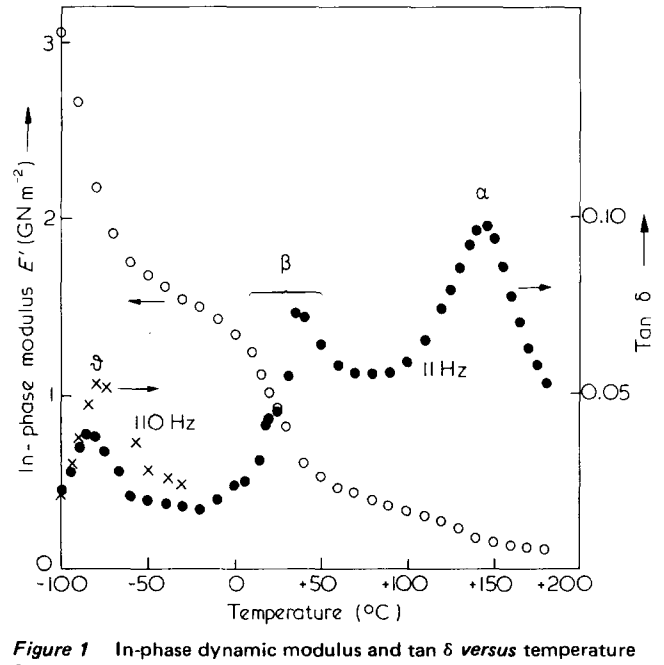

Figure 1 In-phase dynamic modulus and tan δ *versus* temperature for the commercial material at 11 Hz

*Kindly supplied by ICI Plastics Division.

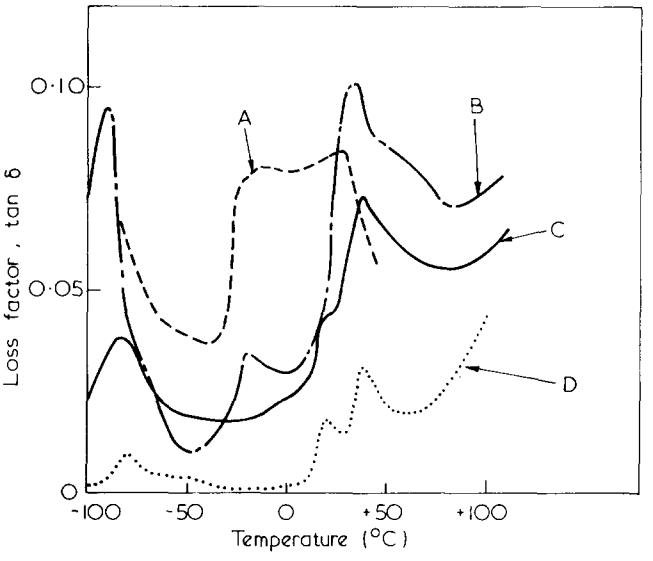

Figure 2 Loss factor for commercial PTFE in simple tension, simple shear and shear yielding. A, Pure shear yielding, 10^{-1} Hz; B, simple shear, tan δ_S, 2 Hz; C, tan δ_T, simple tension, 11 Hz; D, tan δ_V computed

for the β transition. For the γ peak, there is an increase of a factor of three. There is also evidence of an additional process around −20°C which may be linked to the small effect noted at −5°C in the tension data. Since the shear test involves no hydrostatic stress, it is possible to deduce the loss factor for the volumetric deformation, tan δ_V, from those in shear, tan δ_S, and tension, tan δ_T. Taking tan $\delta_S = \mu''/\mu'$, where μ is the shear modulus ($''$ refers to the out-of-phase component, and $'$ to th in-phase), tan $\delta_T = E''/E'$, and noting that $G = E/2(1+\nu)$, we may derive an expression for tan $\delta_V = K''/K'$, where K is the bulk modulus given by $K = E/3(1-2\nu)$. By eliminating the out-of-phase Poisson's ratio, ν'', we have:

$$\tan\delta_V = (1-2\nu')\frac{\tan\delta_T \tan\delta_S}{3\tan\delta_S - 2(1+\nu')\tan\delta_T} \qquad (1)$$

where ν' is the in-phase Poisson's ratio.

Note that for tan δ_T = tan δ_S, tan δ_V = tan δ, and that for $\nu' = \frac{1}{2}$, tan $\delta_V = 0$, since the in-phase component is infinite. In *Figure 2*, tan δ_V is shown computed for $\nu' = 1/3$ (G' and E' gave ν' values in the range 0.15 to 0.25, but these are likely to be very inaccurate), and two peaks are indicated within the β transition which may correspond to the crystal phase changes which are more likely to be reflected in tan δ_V.

An additional series of tests was carried out to measure the stress-strain curves over a range of temperatures at several rates in order to look at larger strain properties. The system of plane strain compression was used, since it is stable,[18] and it gave stress-strain curves of the form shown in *Figure 3*. There is pronounced work-hardening after yielding as indicated by the slope change in the curve. It was found that in common with other polymers,[19] e_y was approximately constant with varying temperature and rate, and here was about 0.045. *Figure 4* shows the lines for three strain rates and there is an abrupt change between 0° and 20°C with a clear rate effect. This can be represented in the form:

$$\sigma_y = \sigma_0 \dot{e}^n \qquad (2)$$

where n is approximately constant. n may be related to the loss factor of the system by considering the response to a

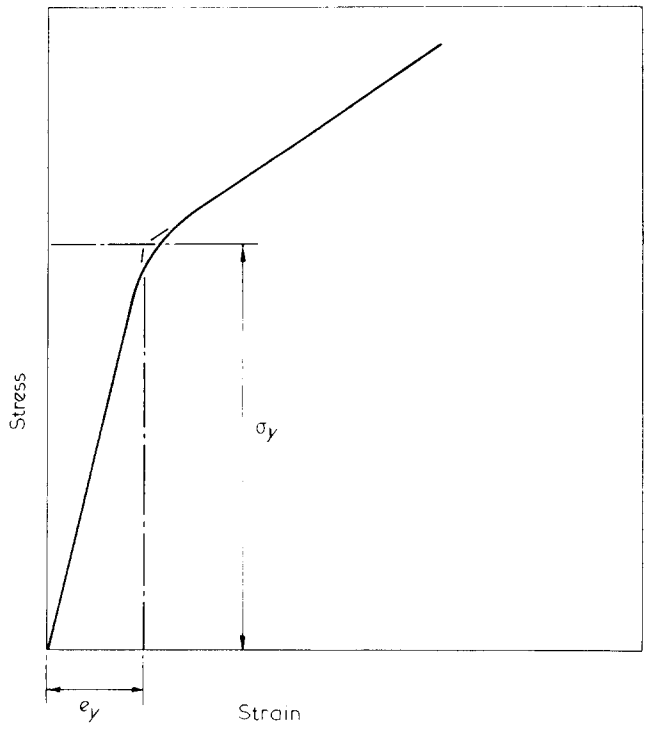

Figure 3 Diagrammatic stress-strain curve for PTFE in plane strain compression

sinusoidal input, which gives the result that $\tan(\pi/2)\,n \simeq \tan\delta$. The values of $n\,(\mathrm{d}\ln\sigma_y/\mathrm{d}\ln\dot{e})$ are shown in *Figure 4* and are also given in *Figure 2* as $\tan\delta$, within the temperature range studied where they can be seen to show a similar pattern to the simple shear elastic data, although they are somewhat higher. The presence of shear processes at -20°C is clearly evident from these results and they indicate an increase in $\tan\delta$ with strains up to yield. However, there was no evidence for strains up to about 50% of any further increase in $\tan\delta$.

Rheovibron loss factor data for the commercial and heat-treated materials are shown in *Figure 5*. Although basically of a similar shape, the curves do indicate slight differences in the behaviour of the three materials. The quenched sample has a higher $\tan\delta$ than the other materials at the α and γ peaks, whereas at the β peak it is found to have the lowest value. The opposite is true of the commercial sample, being low at the α and γ peaks but high at the β peak. This behaviour is consistent with the crystallinity measurements and a knowledge of whether the crystalline or amorphous phase is involved in a particular relaxation. Since the quenched material has the lowest crystallinity, it follows that its reaction at the α and γ peaks, which involve the amorphous phase, should be enhanced. However, a diminished response might be expected at the β peak which involves a crystalline phase change. By a similar argument, one might expect the commercial and slow cooled samples to behave much the same as one another since they are of identical crystallinity, and the curves display few differences.

Figure 6 shows the in-phase dynamic modulus, E', for the three materials. These curves have been corrected for end effects,[16] and again their relationship is sensible, with the quenched, low crystalline sample having the lowest modulus and the slow cooled sample having the highest modulus, an indication of its increased crystallinity.

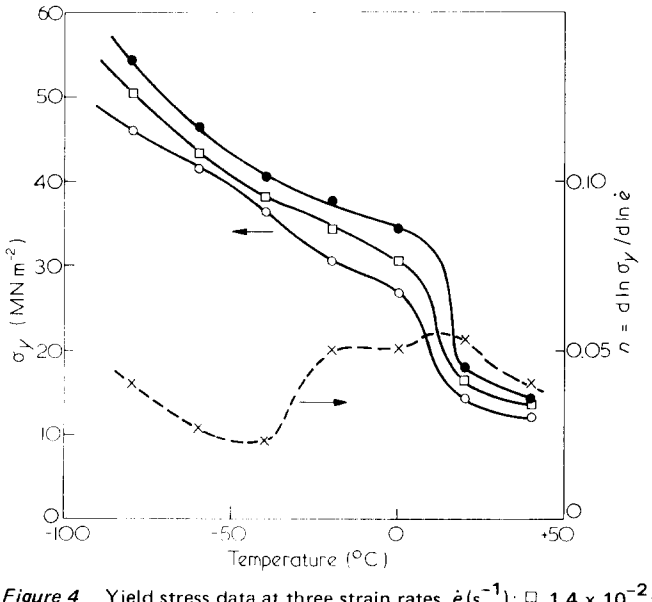

Figure 4 Yield stress data at three strain rates. $\dot{e}\,(s^{-1})$: □, 1.4×10^{-2}; ○, 1.4×10^{-3}; ●, 1.4×10^{-1}

IMPACT TESTING

Analysis

In most impact analyses, the impact strength is defined in terms of the energy required to break a notched specimen expressed as energy per unit of broken ligament area. It has been pointed out[4] that this is not the Griffith condition for initiating a brittle fracture in which the energy per unit area of the fracture surface, G_c, is expressed as a derivative:

$$G_c = \frac{\mathrm{d}U}{\mathrm{d}A} \tag{3}$$

where U is the energy of the system and A is the crack area. The conventional tests use $G_c = U/A \neq \mathrm{d}U/\mathrm{d}A$ unless G_c is constant across the section. The derivative condition can be expressed in terms of the change of the compliance of the specimen, C, with crack area:[4]

$$\frac{\mathrm{d}U}{\mathrm{d}A} = \tfrac{1}{2}P^2\,\frac{\mathrm{d}C}{\mathrm{d}A} \tag{4}$$

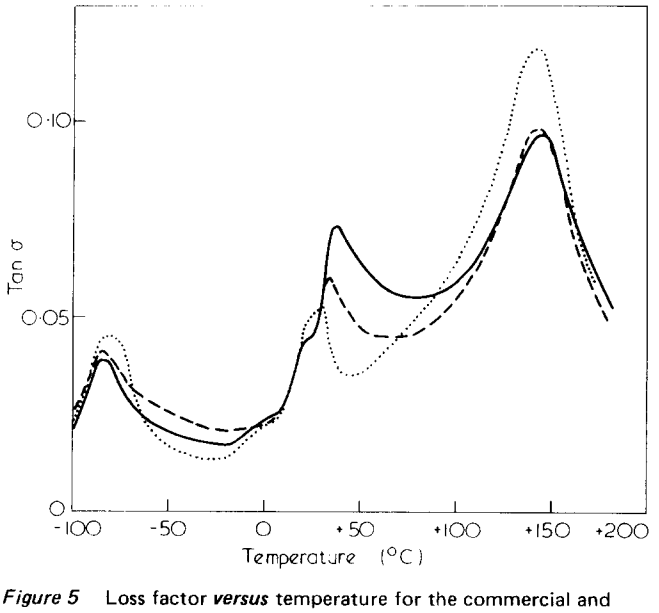

Figure 5 Loss factor *versus* temperature for the commercial and heat treated materials at 11 Hz. ——, Commercial; – – – –, slow cooled; . . . . ., quenched

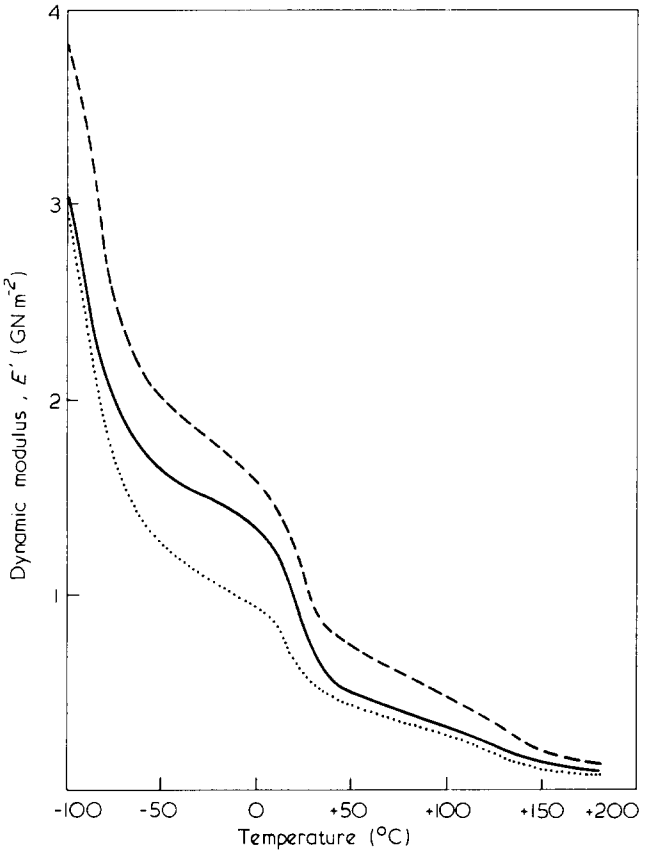

Figure 6 Dynamic modulus *versus* temperature for commercial and heat treated PTFE. ——, Commercial; ——, slow cooled; . . . ., quenched

where P is the load. However, for an elastic system, P may be expressed in terms of the total energy absorbed so that:

$$U = \tfrac{1}{2}P^2C \tag{5}$$

and, by combining these three equations, we have:

$$G_c = U\frac{1}{C}\frac{dC}{dA} \tag{6}$$

For the common rectangular geometry of depth D and breadth B with a through thickness crack of length a, this may be written as:

$$U = G_cBD\phi \tag{7}$$

where $\phi = C/(dC/d(a/D))$, a geometric parameter which may be obtained either experimentally by finding C as a function of a, or by calculation. The Charpy test was used for all the experiments performed here with the geometry shown in *Figure 7a* and for which ϕ has been determined for a range of L/D ratios,[20] and is shown in *Figure 7b*.

G_c may be determined by assuming that the energy measured in the impact test is U so that, since B, D and ϕ are known, G_c is calculated from equation (5). The major error in this assumption is that the measured energy usually includes the kinetic energy of the specimen. This may be removed by testing specimens of different crack lengths and plotting U *versus* $BD\phi$ as shown in *Figure 7c*. G_c may be found from the slope of the line and the kinetic energy is the intercept.

A useful adjunct of this method is that the strain rate of the test may be altered by changing the specimen dimensions since the gross strain rate, $\dot{e}$, for this geometry is:

$$\dot{e} = 6\left(\frac{V}{D}\right)\left(\frac{D}{L}\right)^2 \tag{8}$$

where V is the impact fracture velocity. Changing $\dot{e}$ by varying V is not usually feasible because of the associated energy changes, but variations in L do allow about a factor of 10.[5]

An effect of some importance here is that associated with materials which show either substantial ductility, and hence plastic zones at the crack tip, or those which give slow crack growth prior to final instability. Both will

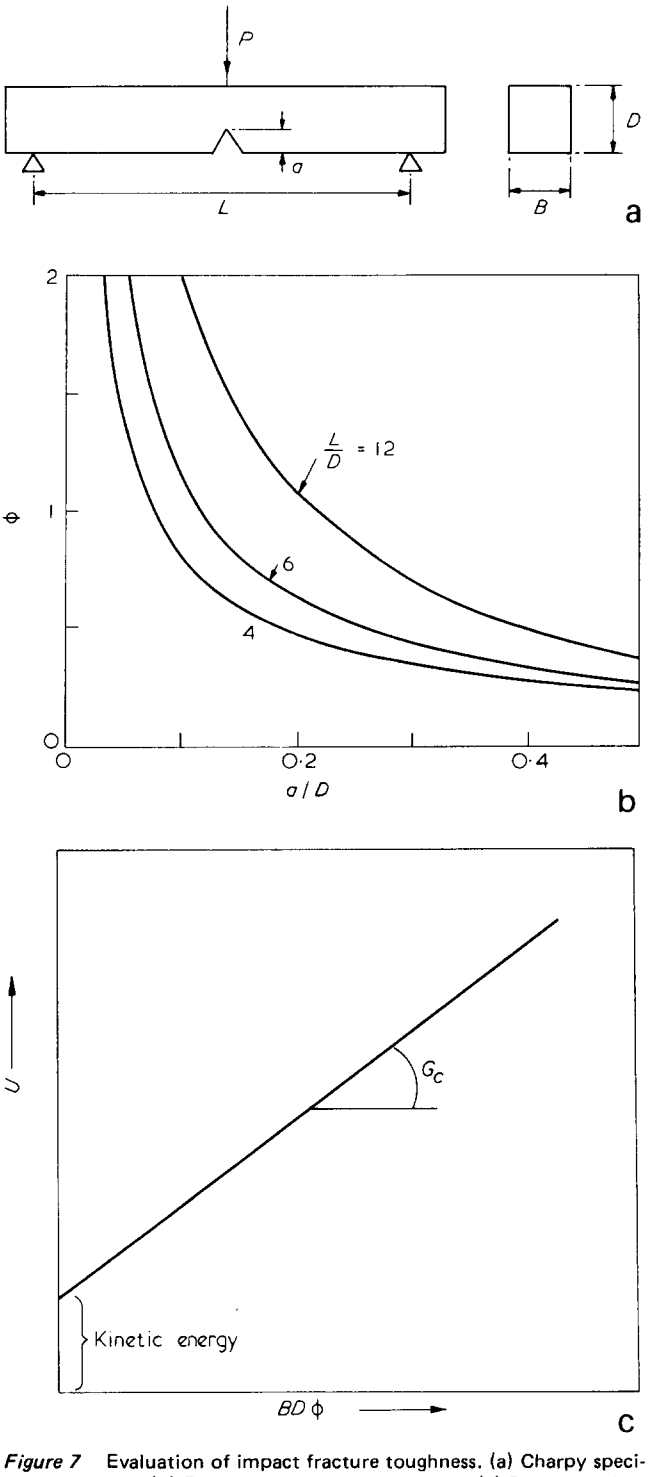

Figure 7 Evaluation of impact fracture toughness. (a) Charpy specimen geometry; (b) Form of calibration parameter; (c) Determination of G_c removing kinetic energy

result in the *U versus* $BD\phi$ graph showing curvature and this may be corrected by adding a length Δa to a until linearity is achieved.[4,5] Which of the two processes is occurring can only be determined by other observations.

Experiments and results

The impact tests were performed on a specially designed, but conventional configuration, pendulum impact tester which had a range of pendulum sizes and a photoelectric angle measuring device to ensure high accuracy.[21] A temperature enclosure for the specimens enabled tests to be carried out over the range -100° to $+170^\circ$C. A typical test consisted of breaking a set of specimens with a range of notch lengths ($0.05 < a/D < 0.5$) machined in with a very sharp fly cutter (tip radius < 2 μm). The recorded energy *versus* $BD\phi$ graph was then drawn to determine the degree of curvature and amount of scatter, and *Figure 8* shows some typical data at two temperatures for $B = D = 6$ mm and $L = 21$ mm.

It can be seen that there is some scatter and curvature is apparent. Several methods of correction were tried and that finally used added increasing values of Δa to the crack length values and used an intercept value of the kinetic energy plus an amount $G_c B \Delta a$, where G_c is the current value. Attempts to use a floating intercept were unsatisfactory with less than about 20 points, although that would clearly be a preferable procedure. The basic kinetic energy value was obtained by impacting an unsupported specimen and it was found that tests which required little or no correction did extrapolate through this value. For those in which a correction was needed, Δa was increased until a minimum

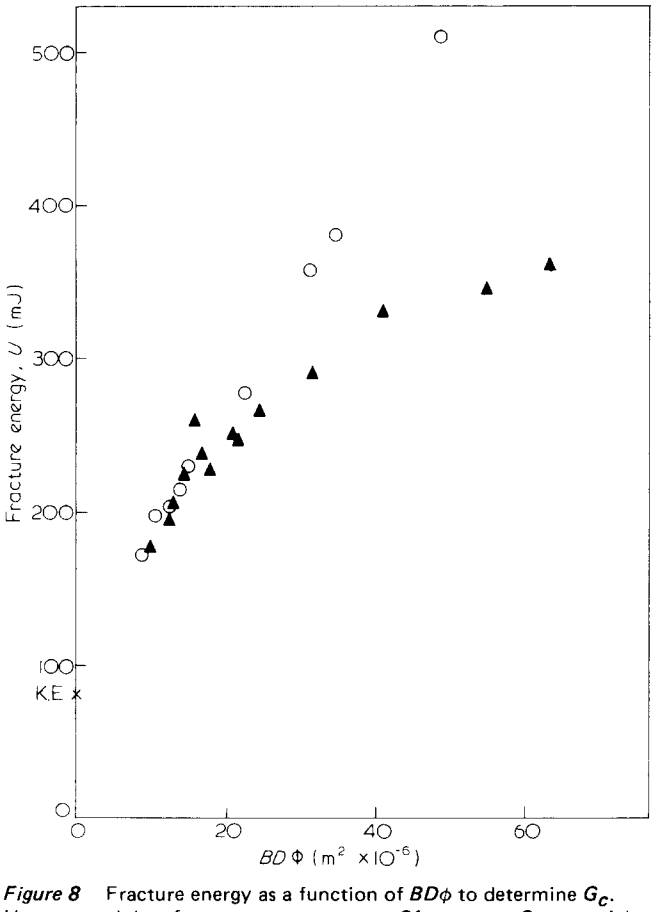

Figure 8 Fracture energy as a function of $BD\phi$ to determine G_c. Unprocessed data for two temperatures at 21mm span. Commercial PTFE: ▲, -100°C, corrected $G_c = 9.22$ kJm^{-2}; ○, 150°C, corrected $G_c = 9.65$ kJm^{-2}

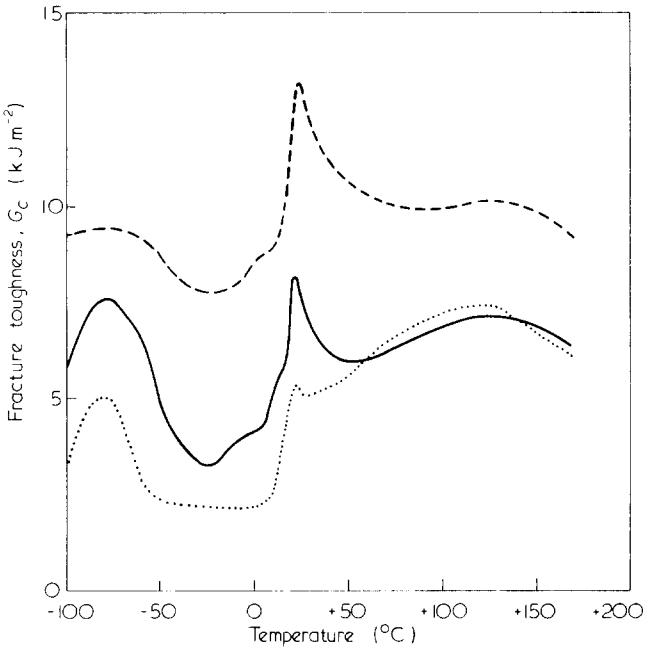

Figure 9 Impact fracture toughness *versus* temperature for three strain rates-commercial material.

Span	Span mm	$\dot{e}(s^{-1})$
-----	21	274
———	41	72
.....	72	23

standard deviation of the points was achieved. Attempts to force the extrapolation of Δa corrected data through the kinetic energy intercept were unsatisfactory, leading to larger Δa corrections than were necessary to give the minimum standard deviation, suggesting that the addition of $G_c B \Delta a$ was valid. An additional observation was that, for tests in which there was a high degree of scatter, Δa tended to increase and also was subject to considerable, apparently random, variation. This suggests that the scatter is due to inconsistencies in notch tip radius which result in different Δa values. The use of the Δa correction procedure did improve the consistency when G_c values were plotted *versus* temperature, for example (see Discussion).

The basic tests were performed on the commercial material using 72, 41 and 21 mm span specimens in which $D = B = 6$ mm, and the resulting G_c *versus* temperature curves are shown in *Figure 9*. These spans correspond to strain rates of 23, 72 and 274 s^{-1}, respectively, for a striker velocity of 3.3 m/s. There is a general pattern of peaks corresponding approximately to those temperatures where loss peaks are observed, but clearly the relative sizes are different for the three strain rates. The 41 mm span results required more correction and were more scattered and since they were the first tests performed, it is believed this resulted from poor notching. The Δa values required are shown *versus* temperature in *Figure 10* and, although there is considerable scatter, it is clear that there are peaks at the same temperature as G_c and $\tan\delta$. The data for the 72 and 21 mm spans show the same pattern, but there were almost no corrections for the 72 mm (< 0.1 mm) and for 21 mm they were around 0.2 mm.

A similar set of tests were performed on the annealed and quenched materials, and the G_c *versus* temperature data are shown in *Figure 11*, together with that for the commercial material. The pattern is basically the same with rather small differences at low temperature, but above

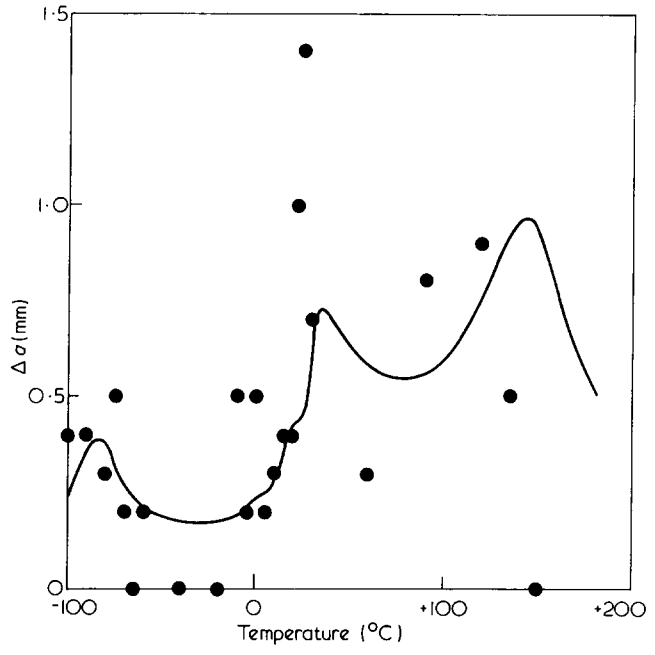

Figure 10 Crack length correction Δa for 41 mm span results. $\Delta a = 10 \tan \delta$

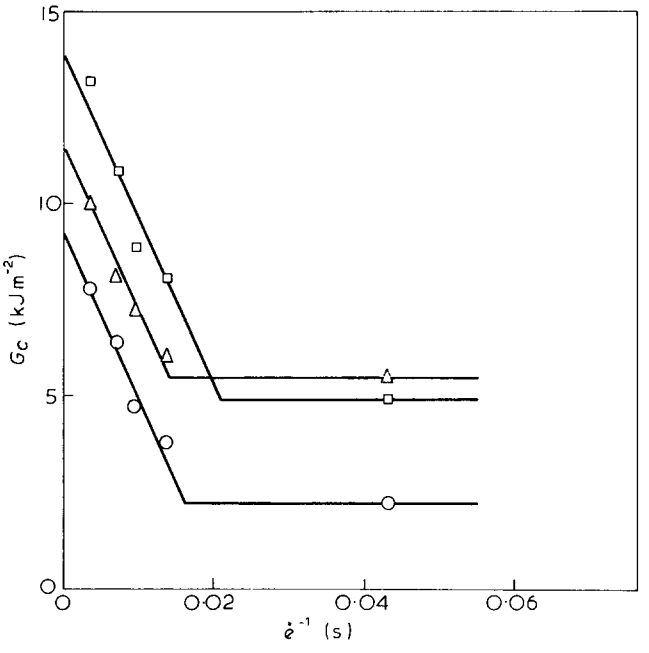

Figure 12 Impact fracture toughness *versus* inverse strain rate (∞ time) for three temperatures–commercial PTFE. ○, − 30°C; □, + 20°C; △, + 50°C

20°C these two materials give markedly higher values.

It is clear from *Figure 9* that there are remarkably high degrees of rate dependence indicated by the differences in the G_c curves, particularly for temperatures below 20°C. Above this value, there is no significant difference between the 72 and 41 mm data, but the 21 mm is higher. These effects have been reported previously[5] for polyethylene and were explored further here in detail at −30°, +20° and +50°C. The rate was changed by altering both D and V in addition to span and for rates greater than 20 s^{-1}, a continuous increase in G_c with $\dot{e}$ was found which could be modelled quite well with power law indices of about 0.5 for the −30° and +20°C data. At +50°C, the values did not increase significantly for $\dot{e} < 100\,s^{-1}$ which confirmed the identity of the 41 and 72 mm data noted previously.

Attempts to relate these large indices to tan δ were unsuccessful and generally reflected the absolute value of G_c. The results shown in *Figure 12* plotted as G_c *versus* $\dot{e}^{-1}$ give good linearity and illustrate a critical cut-off point. The 72 mm data are representative of the low rates and, as $\dot{e} \to \infty (G_0)$, the extrapolated values give an upper bound, the two lines are shown in *Figure 13*. The critical strain rate at which the G_c values change varies somewhat with temperature but is about 60 s^{-1}.

DISCUSSION

The basic question to be answered from these results is that posed by Vincent,[3] i.e. is the energy absorbed in the impact fracture dissipated by the same mechanism as that

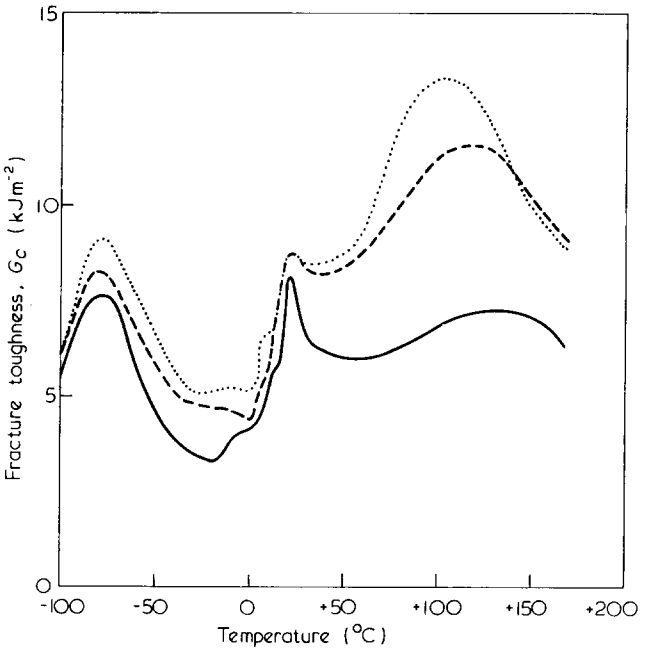

Figure 11 Impact fracture toughness *versus* temperature for commercial and heat treated PTFE, 41 mm span. ——, Commercial; – – – –, slow cooled; . . . . ., quenched

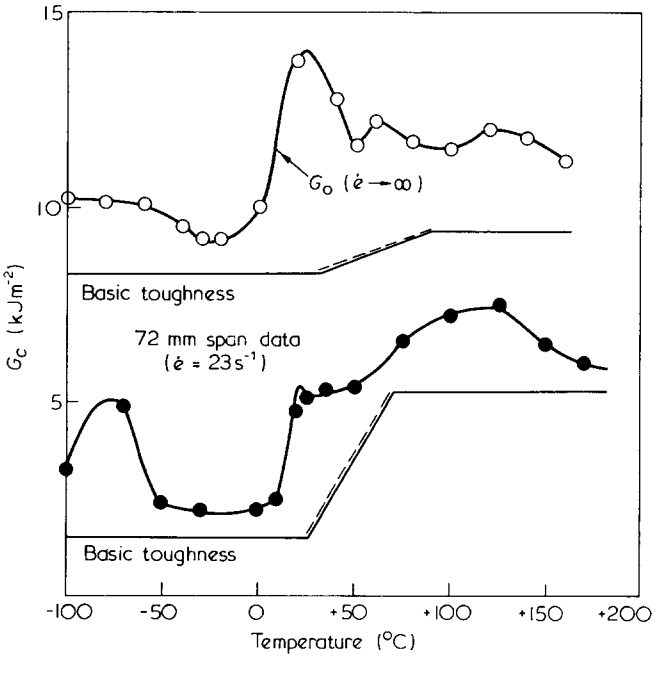

Figure 13 Slow and high rate impact fracture toughness showing derived basic toughness lines–commercial PTFE

which produces viscoelastic losses? In general, the tan δ peaks are less than 10% of the total energy involved so that the substantial impact strength peaks, which are sometimes double the base value, must involve some form of amplification mechanism. This is confirmed by an analysis of fracture recently suggested by Andrews,[22,23] where the fracture energy is related to an hysteresis ratio for each element integrated over the whole specimen. If this ratio were tan δ only, then G would reflect that proportion of the total energy. In fact, the changes are much larger, indicating that the energy loss must be enahnced at least in part of the specimen and this is most likely around the crack tip. Alternatively, it may be that the peaks result from different mechanisms but derive from the same molecular motions of the whole, or some part, of the material.

Reference to the mechanical deformation provides part of this answer in that it is difficult to define the magnitude of tan δ in a given temperature range with any precision. This is because, as pointed out previously, the magnitude and position of the loss peaks will depend on frequency, stress state and deformation amplitude. The equivalent frequency of the fracture will be given by:

$$w \simeq \frac{\dot{e}}{4e_y} \tag{9}$$

so that here they vary between 10^2 and 10^3 Hz. There is some evidence of the impact peaks being at slightly higher temperatures than those for the γ peaks in tan δ but the reverse is true for β and α, sometimes by as much as 30°C (α). The large strains in the notch tip region will induce local yielding which is essentially a shear process so the correlation would be expected to be best with the simple shear data. Both the yield and the simple shear tan δ data in *Figure 2* have peaks in the γ and β regions, but the 0°C to −40°C range gives evidence of a peak which is not seen in the impact data. As a final point, it was noted that there was strong rate dependence in the impact data which seemed to occur for $e > 60\,s^{-1}$ and that this showed no correlation with tan δ. This implied value of this dependence ($n \simeq 0.5$) is of a magnitude not seen in tan δ results, even for very large strains. We are therefore forced to the conclusion that the impact strength peaks are *not* simply the tan δ peaks transposed to some other set of conditions, but are a separate mechanism which relies on the same basic molecular motions.

The identity of this separate mechanism is particularly difficult to determine for a material of complex structure such as PTFE. There is a basic pattern of behaviour which seems typical of most polymers under impact conditions[21] which may be described in terms of two, temperature independent, values of G_c. One, G_{c1}, is associated with the constrained region near the centre of the specimen where plane strain exists, and the other, G_{c2}, occurs in the plane stress regions near the surfaces. In general, the rates in the impact tests are sufficiently high that these values are independent of temperature, as is the modulus, E, associated with them. The extent of the plane stress zones are given by:

$$r_{p_2} = \frac{EG_{c2}}{2\pi\sigma_y^2} \tag{10}$$

so that the average value of G_c, G_c', at any temperature is given by:

$$G_c' = G_{c1} + \frac{EG_{c2}}{\pi\sigma_y^2 B}(G_{c2} - G_{c1}) \tag{11}$$

Now, $G_c' = G_{c2}$ when $r_{p_2} = B/2$, i.e. when the plane stress region is fully across the specimen so that a transition from G_{c2} at high temperatures to G_{c1} at low temperatures would be expected. The temperature where this transition occurs will depend on σ_y and B, and we can see from *Figure 4* that σ_y changes from about 10 to 30 MN/m² from +20° to 0°C. Using $E \simeq 1$ GN/m² and $G_{c2} \simeq 5$ kJ/m² gives r_{p_2} values changing from 4 to 1 mm, indicating that the transition would be expected in this range. Certainly, the 72 mm span G_c values in *Figure 13* show a marked decrease but the situation is complicated by the presence of peaks in G_c, particularly that for the β transition.

Clarification is provided by assuming that the energy absorption processes associated with the peaks are separate, and quite distinct, from the basic process outlined above. If both the tan δ loss process and the impact energy mechanism are assumed to arise from the same portion of material, then the energy would be expected to be proportional to tan δ. There are problems with the peaks not coinciding, as mentioned previously, but if the tan δ and G_c graphs are displaced to give coincident peaks in each transition region, then graphs of G_c *versus* tan δ may be plotted for each transition and these are shown for the 72 mm span and for G_0 in *Figure 14*, using the simple tension tan δ results. There are quite good lines for each relaxation peak and both the β and γ give the same intercept for each set of results. The slopes are very similar for the α and γ peaks but that for β does increase from the 72 mm data to those for G_0. There are a group of points between the α and β peaks which do not lie on either line and these represent those which are on the overlap between the α and β peaks. The basic toughness lines given by the intercepts are shown in *Figure 13* and the broken lines indicate the expected

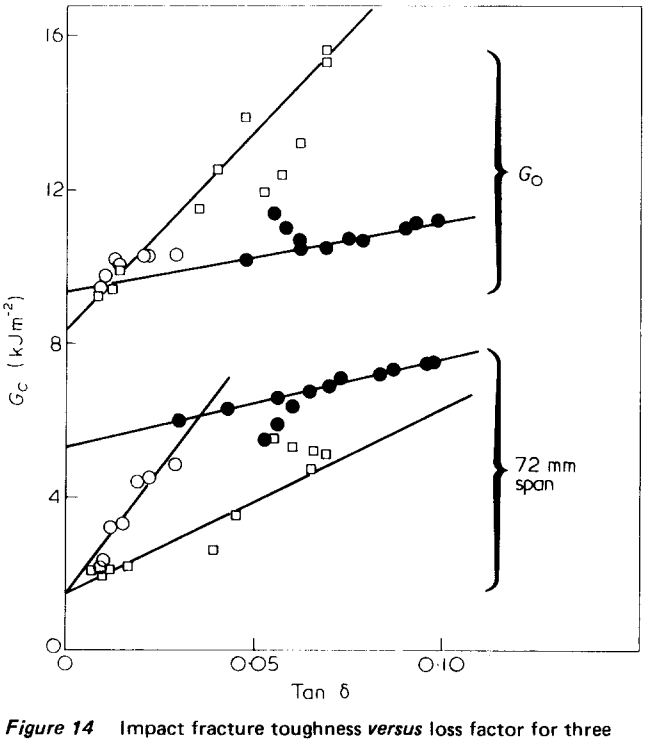

Figure 14 Impact fracture toughness *versus* loss factor for three transitions at high and low rates, commercial material. ●, α, □, β; ○, γ

transition regions. For the materials with different heat treatments, there is very little difference in the β and γ regions, but for the α there is sufficient difference to warrant investigation. *Figure 15* shows G_c as a function of tan δ for the three materials and a common intercept is given but with a higher slope for the heat-treated samples. In fact, this slope is much closer to those of the β and γ peaks, suggesting a much closer similarity of behaviour of the three peaks for these materials.

The basic toughness curves are, therefore, of the form expected with a transition from G_{c1} to G_{c2}. For strain rates below about 60 s^{-1}, the values remain constant at 1.5 and 5.3 kJ/m^2, respectively, but above this rate there is a rapid increase to values of about 9 kJ/m^2 and a much smaller difference between G_{c1} and G_{c2}. The molecular processes governing these changes are unlikely to be those associated with the loss and impact strength peaks since they are largely unchanged. It seems more likely, therefore, that they are governed by main chain motions which are reflected in shear yielding since these will determine both the values of G_{c1} and G_{c2} and their relative proportions. One would therefore expect abrupt changes in shear yielding behaviour in the same strain rate regimes but, although such changes have been reported,[24] there is some doubt as to their magnitude.[25] The change in relative values of G_{c1} and G_{c2} also implies rapid changes in Poisson's ratio since their ratio is controlled by volume constraint. If the rate effect is associated with gross yielding, then there is no reason to expect it to be rare and, indeed, it has been observed in impact data for polyethylene (both MD and HD) and for PMMA. Attempts to attribute the effect to a range of experimental artefacts have all failed and it is the authors' belief that it is a genuine effect.

The physical origin of such a rapid rate change is hard to establish. Double logarithmic plots suggest power-laws of the order of 0.5 and, indeed, surface markings in MDPE showed this dependence[5] which might suggest some form of diffusion-controlled process. Diffusion of external environments on this time scale are difficult to visualize and

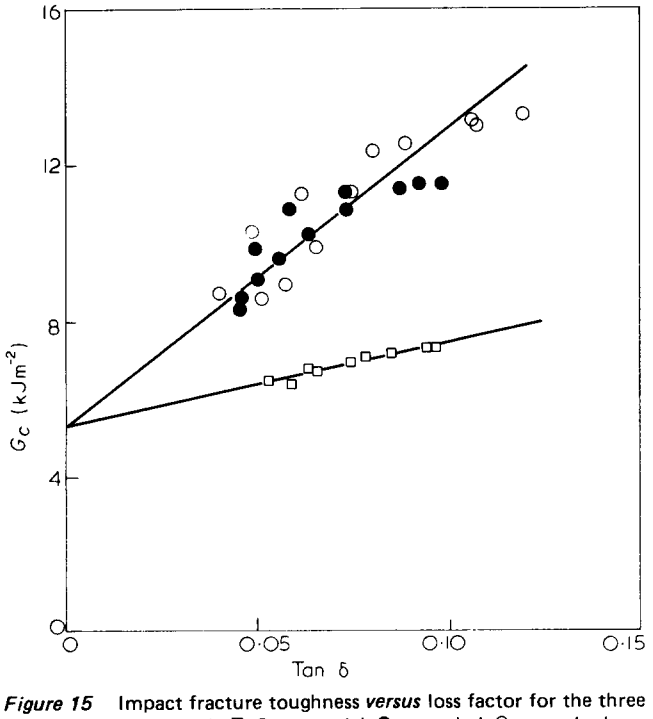

Figure 15 Impact fracture toughness *versus* loss factor for the three PTFE materials–α peak. □, Commercial; ●, annealed; ○, quenched

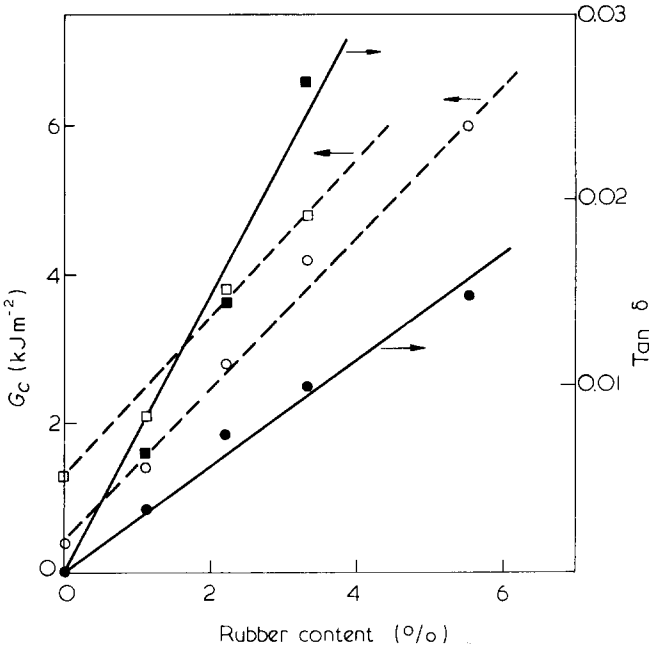

Figure 16 Impact fracture toughness at + 20°C, and loss peak at − 80°C *versus* rubber content for modified polystyrene resins

attempts to exclude the atmosphere produced no effect. The time scales of these tests (≅ 1 ms) are such that there is likely to be adiabatic heating at the crack tip region during crack initiation and the propagation of heat from the crack tip would be governed by a relationship of the form observed. Indeed, it is feasible that the temperature rise in the crack tip region would be sufficient to elevate the material locally to the glass transition temperature, thus giving the possibility of additional energy absorption by flow processes. G_0 would therefore represent an adiabatic toughness at crack initiation.[29]

The mechanism which results in the increase in G_c at the loss peaks and which is superimposed on the basic yeilding of the material is probably that of the generation of multiple crazes, which would be consistent with it being associated with some portion of the material. In addition, the stable growth of crazes requires loss processes in order to operate so that the presence of a loss peak would certainly be conducive to craze formation and the consequential energy absorption. There is also supporting evidence for this contention from other materials. In PMMA, there is a peak in impact strength at its β peak only for blunt notches where multiple crazes form.[21] In rubber-modified polystyrene, the addition of rubber increases the low temperature loss peak and also the impact strength at all temperatures, largely by the induction of numbers of crazes which manifest themselves by general whitening.[26, 27] Indeed, both tan δ and G_c are proportional to rubber content here (although at different temperatures) and so there is a resulting linearity between G_c and tan δ as for PTFE. *Figure 16* shows both G_c and tan δ as functions of rubber content for two back-blended sets of resins using different basic polystyrenes.[27] The intercepts (for zero rubber content) are different, as expected, but the increase with rubber content is the same, indicating that the additional crazing energy is a function of the number of rubber particles, but is not strongly influenced by nature of the basic material. Tan δ, on the other hand, is strongly dependent on the type of resin used. The resulting cross plots are shown in *Figure 17* and give similar lines to those for PTFE, although the slopes are much larger here.

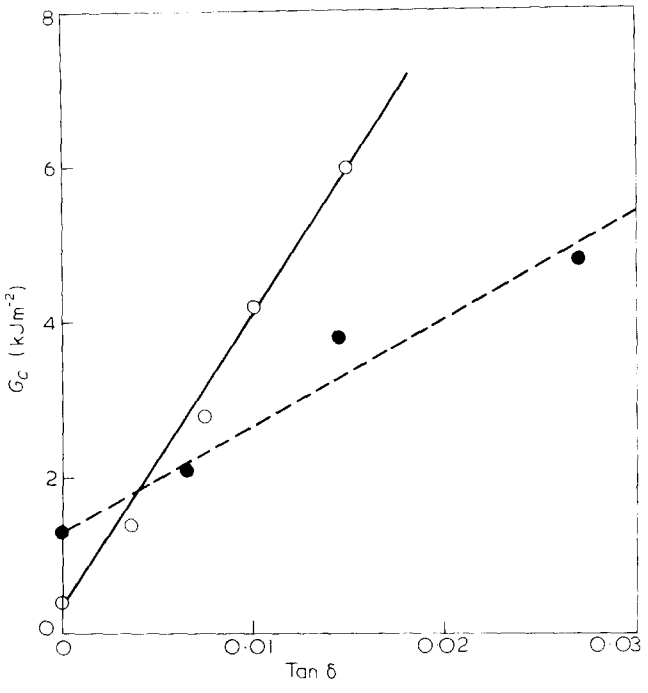

Figure 17 Impact fracture toughness *versus* loss factor for rubber modified polystyrene

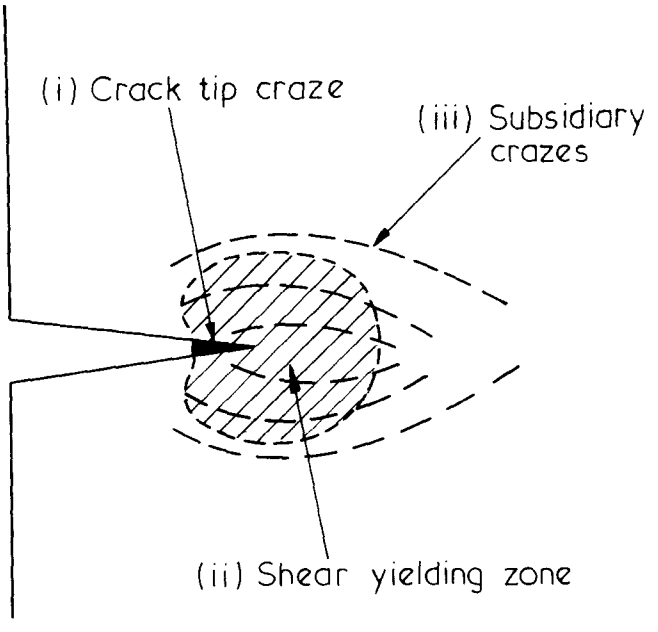

Figure 18 Three mechanisms for energy absorption

The effects of correction length, Δa, shown in *Figure 10*, also fall within this general framework since, if the correction is regarded as a measure of the size of the additional crazed zone, then Δa would be proportional to the additional part of G_c. This, in turn, is proportional to tan δ so that we have:

$$\Delta a \cong \frac{1}{2\pi} \frac{E\Delta G_c}{\sigma_y^2} = \text{constant} \times \tan \delta$$

where ΔG_c arises from the multiple crazing. The constant would be about 10 mm, using typical values of the parameters, and the line in *Figure 10* is derived using that value and and tan δ_T taken from *Figure 1*. This would also explain why poor notching gave larger Δa values since such notches tend to give more crazing, an effect noted in many other testing situations (e.g. ref 28). The addition of $G_c B \Delta a$ to the kinetic energy used in the correction procedure probably gives a measure of the additional energy absorbed in the craze craze zone.

CONCLUSIONS

The question originally posed has not been answered completely here, but ther is good evidence on which to base the proposed model of the behaviour. It is suggested that there are three energy absorbing processes occurring in the crack tip region in an impact test which are illustrated in *Figure 18*.

(i) There is a large single craze at the tip of the crack which controls the energy absorption in the highly constrained plane strain stress state. Such crazes require a high hydrostatic stress component in order to form and this is always present for sharp cracks (G_{c1}).

(ii) Shear yielding can occur (shown shaded) which enhances the energy absorption of the craze, but only occurs when there is freedom for shear deformation, as near the specimen surfaces (G_{c2}).

(iii) Subsidiary crazes can occur around the crack tip providing there are sites at which they can form a stabilizing viscoelastic mechanism to enable them to grow. Processes (i) and (ii) are apparently highly rate dependent above a strain rate of about 60 s^{-1} and the mechanism is probably that of local adiabatic heating. Process (iii) superimposes onto the other two and may be regarded as an additional, separate mechanism.

REFERENCES

1 Heijoer, J. *J Polym Sci* 1968, **16**(7), 3755
2 Boyer, R.F. *Polym Eng Sci* 1968, **8**, 161
3 Vincent, P.I. *Polymer* 1974, **15**(2), 111
4 Williams, J.G. and Birch, M.W. *Proc 4th Int Conf on Fracture* 1977, **1**(IV), 501
5 Birch, M.W. and Williams, J.G. *Int J Fracture* 1978, **14**, 69
6 Quinn, F.A., Roberts, D.E. and Work, R.N. *J Appl Phys* 1951, **22**(8), 1085
7 Rigby, H.A. and Bunn, C.W. *Nature* 1949, **164**(4170), 583
8 Bunn, C.W. and Holmes, D.R. *Discuss Faraday Soc* 1958, **25**, 95
9 Miller, R.G.J. and Willis, H.A. *J Polym Sci* 1956, **19**, 485
10 Moynihan, R.E. *J Am Chem Soc* 1959, **81**, 1045
11 McCrum, N.G., Read, B.E. and Williams, G. 'Anelastic and Dielectric Effects in Polymeric Solids', Wiley, New York-London, 1967
12 McCrum, N.G. *J Polym Sci* 1959, **34**, 355
13 Ohzawa, Y. and Wada, Y. *Rep Prog Poly Phys Jpn* 1963, **6**, 147
14 Satokawa, T. and Koizumi, S. *J Chem Soc Jpn, Ind Chem Sect* 1962, **65**, 1211
15 Krum, F. and Müller, F.H. *Kolloid Z* 1959, **164**, 8
16 Hodgkinson, J.M. to be published
17 Kabin, S.P. *Sov Phys Tech Phys* 1956, **1**, 2542
18 Williams, J.G. *Trans J Plast Inst* June 1967, 505
19 Williams, J.G. *Int J Fract Mech* 1972, **8**(4), 393
20 Plati, E. and Williams, J.G. *Polym Eng Sci* 1975, **15**(6), 470
21 Plati, E. and Williams, J.G. *Polymer* 1975, **16**(12), 915
22 Andrews, E.H. *J Mater Sci* 1974, **9**, 887
23 Andrews, E.H. *J Mater Sci* 1977, **12**, 1307
24 Briscoe, B.J. and Hutchings, I.M. *Polymer* 1976, **17**(12), 1099
25 Briscoe, B.J. private communication
26 Nikpur, K and Williams, J.G. *Plast Rubber: Mater Appl* November 1978, 163
27 Nikpur, K. 'The Effect of Rubber Content on the Strength of Impact Polystyrene', *PhD Thesis*, University of London (1978)
28 Marshall, G.P., Culver, L.E. and Williams, J.G. *Int J Fract Mech* 1973, **9**(3), 295
29 Hodgkinson, J.M. and Williams, J.G. paper to be presented at *4th Int Conf on Deformation, Yield & Fracture of Polymers, Churchhill College, Cambridge*, 2-5 April 1979